Photoplethysmography Signals and their Correlation with Peripheral Artery Disease

Ava J. Fascetti
The Design Lab
Electrical and Computer Engineering
University of California San Diego
San Diego, CA, USA
afascetti@ucsd.edu

Mustafa H. Naguib
School of Medicine
University of California San Diego
San Diego, CA, USA
mhnaguib@health.ucsd.edu

Elsie G. Ross, MD
Division of Vascular Surgery
Department of Surgery
University of California San Diego
San Diego, CA, USA
e5ross@health.ucsd.edu

Chris Longhurst, MD
Department of Medicine
University of California San Diego
San Diego, CA, USA
clonghurst@health.ucsd.edu

Pam R. Taub, MD
Division of Cardiology
Department of Medicine
University of California San Diego
San Diego, CA, USA
ptaub@health.ucsd.edu

Shamim Nemati, PhD
Department of Biomedical Informatics
University of California San Diego
San Diego, CA, USA
snemati@health.ucsd.edu

Edward J. Wang, PhD
The Design Lab
Electrical and Computer Engineering
University of California San Diego
San Diego, CA, USA
ejaywang@ucsd.edu

Mattheus Ramsis, MD
Division of Cardiology
Department of Medicine
University of California San Diego
San Diego, CA, USA
mramsis@health.ucsd.edu

***Abstract*—Peripheral Artery Disease (PAD) is a common atherosclerotic condition that is underdiagnosed due to the lack of accessible screening options. Photoplethysmography (PPG) serves as a potentially valuable tool in accessible screening for PAD due to its ubiquitous nature and ability to be measured on a smartphone. However, the relationship between PPG and PAD is underexplored. In this paper, we seek to identify features of a PPG signal that correlate with PAD. In an analysis of 5,237 legs from N=2,362 unique patients, we find significant correlations with multiple different features and the ankle-brachial index (ABI), which is used to diagnose PAD. Additionally, these features agree with physiological explanations of PAD and how the disease affects blood flow. These results set up the ability of future work to develop an accessible screening tool for PAD that uses physiologically relevant features of PPG morphology.**

***Index Terms*—cardiovascular health, atherosclerosis, PPG, featurization**

I. Introduction

Peripheral Artery Disease (PAD), a circulatory condition in which narrowed arteries reduce blood flow to the extremities, affects nearly 8 million Americans and 200 million adults worldwide; PAD increases the risk of limb loss along with major adverse cardiovascular events that significantly reduce life quality and expectancy [1]–[3]. The gold standard diagnosis of PAD involves a noninvasive ankle-brachial index (ABI) performed in specialized facilities. The ABI is calculated for each leg as the ratio of the blood pressure in the arteries between the ankle and the arm.

PAD is an underdiagnosed condition, with most patients diagnosed at a more advanced stage of disease. This is especially apparent among high-risk populations where health disparities exist, leading to substantial medical and financial burdens for patients and the US healthcare system [3]–[5]. Consequently, PAD disproportionally affects underserved populations, including minorities, where there is a rising incidence rate of lower extremity amputations [3], [6]. Given the lack of widespread innovations to improve the detection of PAD (to avoid traveling to specialized clinics for ABI screenings), particularly in underserved communities, there exists an unmet clinical need to develop accessible PAD screening alternatives.

Photoplethysmography (PPG) is a non-invasive, simple, cost-effective, optical technique that detects blood flow changes through a vascular bed available on smartphones and non-invasive wearable devices [7]. By shining light into tissue, such as the fingertip or toe tip, and quantifying the backscattered light that corresponds with changes in blood volume, smartphone-based PPG algorithms are well positioned to capture the multifactorial endovascular sequelae of cardiovascular disease, including metabolic changes, endothelial dysfunction, and vascular tone [8]. As such, PPG technologies have been utilized to detect chronic cardiovascular conditions including hypertension and atrial fibrillation [9], [10]. Since smartphone-based PPG measurements are generally understood to be a

Research supported by the American College of Cardiology Foundation, Accreditation Foundation Committee.

reliable methodology with excellent PPG capturing capabilities [11], this provides a promising avenue for making PAD screening more ubiquitous and accessible.

Previous work by Allen et al. has explored the potential for deep learning to detect PAD from PPG signals. However, this work was limited to 214 people and used minutes-long PPG signals [12]. Additionally, the deep learning approach used is not transparent in what aspects of the PPG signal correlate with the presence of PAD. As such, the direct relationship between PPG signals and PAD is still underexplored.

In this work, we explore the relationship between PPG signals and PAD across a large, diverse cohort to unpack what features of PPG signals correlate with a PAD clinical diagnosis. By uncovering the specific PPG pulse morphologies that correlate with disease state (determined by the ABI clinical gold standard), we provide necessary physiological explanations. This brings much-needed transparency to the understanding of the relationship between PPG and PAD, and sets up the physiological basis for future PAD screening algorithms.

II. Methods

This retrospective data analysis study used data collected from patients who presented for a clinically indicated ABI assessment at the University of California San Diego La Jolla or Hillcrest locations between 2020 and 2025. As part of a routine ABI assessment, PPG signals are collected at each toe, and blood pressure (BP) readings are taken at various sites of the body. For each leg for each patient, an ABI value is calculated using the collected BP readings during the assessment. Note that two different company's equipment is used at each location, and as such the PPG capturing mechanisms are different. Therefore, the presented data spans across two datasets of patients. All PPG samples used in analysis are four seconds long.

The population of patients in La Jolla is N=2,400 and in Hillcrest is N=1,319. These datasets combine to give N=3,354 unique patients for analysis (some are shared across dataset). Across the combined dataset, 25% is Hispanic, the average age is 68, 35% has an ABI less than 0.9 (i.e., PAD), and 1% have an ABI greater than 1.4 (i.e., non-compressible).

The featurization pipeline is consistent across datasets. First, the signals are preprocessed. The two datasets are sampled at different frequencies. Therefore, both sets of signals are resampled such that it matches the lower resolution of 75 Hz (the higher resolution dataset has 125 Hz). Next, both sets of signals are band-pass filtered such that only frequencies in the range of 0.5 Hz and 8 Hz remain in the signal. This frequency range was selected to filter out artifact noise from breathing or other movements, as well as high frequency noise from sensing equipment.

After filtering, both sets of signals are passed through a data cleaning pipeline to discard signals that are deemed too noisy for appropriate analysis. Signals are discarded if the main frequency components of the signal are outside the physiological expected range for heart rate. With not all patients having two legs included in the analysis and some having repeat measurements, the total number of signals sent into this pipeline from the unique 3,354 patients is 7,445 signals. Approximately 26 percent of these signals are deemed too noisy for featurization and others lack tabulated BP data, and as such, 5,237 total PPG signals are used moving forward for analysis from N=2,362 unique patients.

To generate features for each PPG signal, one representative pulse per four-second PPG signal is generated. This one pulse is normalized in height and relative time. Features of amplitude and time are calculated prior to normalization to preserve the raw morphology of the pulse. All other features are calculated after normalization. Features in seven different general categories were constructed: rise features, fall features, derivative features, width features, symmetry features, miscellaneous features (e.g., area under the curve), and TSFEL features. TSFEL features are generated automatically using Python's Time Series Feature Extraction Library. Fig. 1 shows some example features; note that these help to visualize the features used in the presented results.

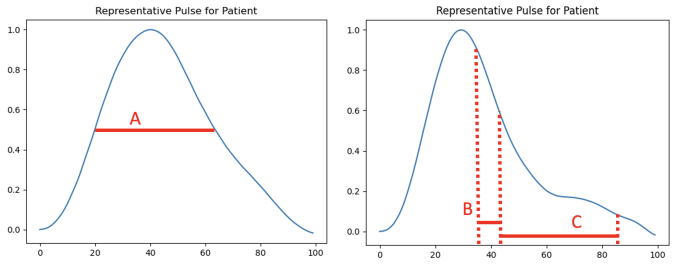

Fig. 1. Three sample features visualized on two normalized PPG pulses. A) Normalized width at half amplitude feature. B) Normalized fall percent time from 90 to 60 percent amplitude. C) Normalized fall percent time from 60 to 10 percent amplitude.

With all features computed, they can be directly compared against that PPG signal's associated ABI measurement. As such, each data point in the results graphs corresponds to one PPG signal (in other words, one patient's right or left leg). As PAD can manifest in one leg and not the other, it is appropriate to treat each leg as a separate data point.

III. Results

Presented below are the correlation plots between specific features of the PPG signal and ABI. Note that hundreds of features were calculated so it is impracticable to present most of them. As such, we pick out noteworthy examples for discussion.

Fig. 2 presents the correlation between the 'normalized width at half amplitude' feature and ABI for the combined dataset of 5,237 clean pulses from N=2,362 patients. Each data point represents an individual's right or left leg, where the x-axis denotes the leg's ABI measurement, and the y-axis denotes that PPG pulse's normalized width at half amplitude value. Data points are color-coordinated for disease level. Individuals with an ABI of greater than 1.0 are healthy. Borderline PAD is classified as ABI values between 0.9 and

1.0. Likely PAD is classified as ABI between 0.7 and 0.9, and severe PAD is classified as ABI values below 0.7.

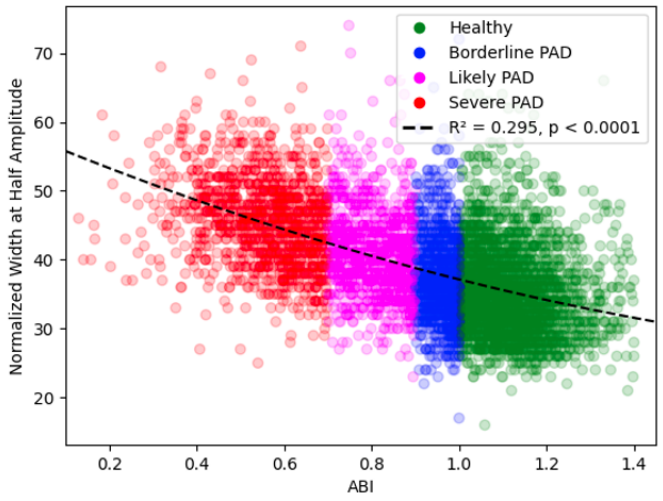

Fig. 2. The PPG feature of normalized width at half amplitude time has a statistically significant correlation with ABI for N=2,362 unique individuals.

Fig. 3 presents the correlation between the 'maximum rising slope' feature and ABI for the same dataset of 5,237 clean pulses from N=2,362 patients. Data points are colored as described previously.

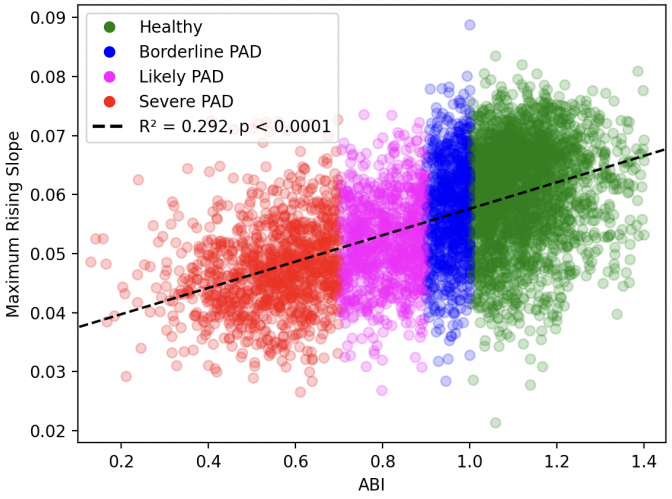

Fig. 3. The PPG feature of maximum rising slope has a statistically significant correlation with ABI for N=2,362 unique individuals.

Fig. 4 presents the results of three different falling edge features. Specifically, the feature of 'normalized fall percent time' was computed for three segments of the falling edge. In the upper left is the time for the pulse to fall from 90 percent amplitude to 60 percent amplitude. In the upper right, from 60 percent amplitude to zero, and in the bottom, from 80 percent amplitude to 10 percent amplitude. In other words, the results show the correlation of fall time at the beginning of the fall, the end of the fall, and throughout the entire fall, against ABI.

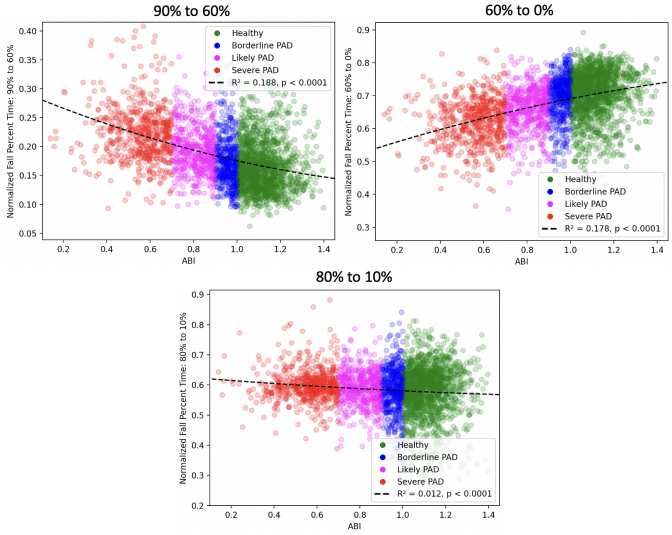

Fig. 4. The PPG features of normalized fall percent time across different segments have different correlations with ABI for N=2,362 unique individuals. (Top left) Fall percent time from 90 to 60 percent. (Top right) Fall percent time from 60 to 0 percent. (Bottom) Fall percent time from 80 to 10 percent.

Lastly, Fig. 5 presents the same correlation as in Fig. 3, where the 'maximum rising slope' feature is correlated with ABI. Here, the data points are color coded for the given site location to show the correlation results from the La Jolla (blue) and Hillcrest (orange) sites.

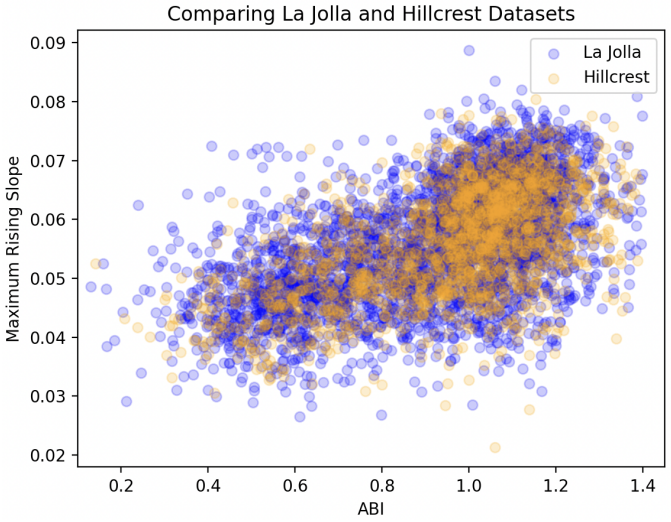

Fig. 5. The correlation between the PPG feature of maximum rising slope and ABI is compared for each dataset. Data from the La Jolla location is shown in blue (N=3,424), and data from the Hillcrest location is shown in orange (N=1,813).

IV. Discussion

These results demonstrate our ability to extract PAD specific morphology features from PPG signals. Fig. 5 verifies that the given pipeline and results are not dependent on a specific dataset or piece of sensing equipment as the features are

consistent across site location. Additionally, it is important to highlight why the given correlations agree with the physiological explanations of PAD. As such, next is a discussion as to why each presented feature agrees with the physiology.

When a patient has PAD, their blood flow to the limbs is reduced due to plaque buildup in their blood vessels. As such, with restricted blood flow and less elastic arteries, the PPG signal becomes more dampened and less defined in shape. A healthy signal is characterized by a steep systolic upstroke and the presence of a dicrotic notch. In individuals with stiffer arteries, the PPG morphology is less specifically defined as the blood reflections at different stages in the cardiac cycle blend together. With this understanding, we can explain the correlations seen in PPG features across ABI value.

Fig. 2 demonstrates that healthier patients (larger ABI values) have smaller widths at half amplitude than patients with PAD. This agrees with the aforementioned description as the PPG signal of a healthy patient has a defined, quicker rising and falling period than a patient with stiffer arteries in which the blood flow through the vessels is more prolonged.

Similarly, Fig. 3 shows that the maximum slope of the systolic upstroke is larger for healthy patients compared to patients with PAD. This concurs with the concept of healthy signals having a faster, defined rising edge.

Finally, the analysis of the PPG falling edge in Fig. 4 provides a more complicated insight. As shown, the correlation of PPG falling time with ABI changes relationship depending on what segment of the falling edge is under analysis. Specifically, our results show that healthy patients have a faster falling edge closer towards the peak of the signal, yet a slower falling edge near the base of the signal, when compared to PAD. In other words, healthy pulses fall faster at first, and slower at the end. This is due to the elasticity of healthy arteries and their ability to reflect the distinct phases of the cardiac cycle. As such, before any reflections reach the extremity, the PPG signal drops quickly from the systolic peak. However, the relative amplitude is prolonged as the elastic arteries reflect the different phases of the cardiac cycle. In unhealthy signals, the reflections all morph together, the signal does not drop quickly from its peak, and there is no distinct trailing edge apart from the end of the cardiac cycle and the end of the PPG signal. Therefore, looking across the entire falling edge of the signal does not reveal a correlation with PAD (as seen in the bottom plot of Fig. 4), but looking at just the top or bottom of the falling edge does.

These insights enable future work to perform a comprehensive analysis of these informative features. Further, future model development can become more transparent by using explicit features of PPG signals to predict PAD, rather than a black-box approach.

It is important to highlight some limitations of the presented work. First, about a quarter of the PPG signals were excluded prior to analysis due to the low quality of the toe PPG signals. This may limit future models in their ability to perform on messy signals. In addition, all of the PPG signals used in this work were obtained by specialists in a clinical setting. Future work is required to validate the correlations and future model performance with smartphone-obtained PPG signals.

V. Conclusion

In this paper, we identify PPG morphology features that correlate with PAD, using the diagnostic metric of ABI, in an analysis of N=2,362 unique patients (5,237 right/left legs). Further, we provide physiological explanations for each presented significant correlation and how our findings agree with the fundamental processes that define PAD. These findings enable future work to focus on using the presented correlative PPG features in the development of a screening algorithm for PAD that is grounded in physiological meaning. By training a model to screen for PAD with just a PPG signal, we can enable accessible screening for PAD to help alleviate the current disproportionate affects of PAD across communities.

References

[1] F. G. R. Fowkes *et al.*, "Comparison of global estimates of prevalence and risk factors for peripheral artery disease in 2000 and 2010: a systematic review and analysis," *The Lancet*, vol. 382, no. 9901, pp. 1329–1340, Oct. 2013. [Online]. Available: https://linkinghub.elsevier.com/retrieve/pii/S0140673613612490

[2] C. W. Tsao *et al.*, "Heart disease and stroke statistics—2022 update: a report from the American Heart Association," *Circulation*, vol. 145, no. 8, Feb. 2022. [Online]. Available: https://www.ahajournals.org/doi/10.1161/CIR.0000000000001052

[3] M. A. Allison *et al.*, "Ethnic-specific prevalence of peripheral arterial disease in the United States," *American Journal of Preventive Medicine*, vol. 32, no. 4, pp. 328–333, Apr. 2007. [Online]. Available: https://linkinghub.elsevier.com/retrieve/pii/S0749379706005587

[4] A. T. Hirsch, "Peripheral arterial disease detection, awareness, and treatment in primary care," *JAMA*, vol. 286, no. 11, p. 1317, Sep. 2001. [Online]. Available: http://jama.jamanetwork.com/article.aspx?doi=10.1001/jama.286.11.1317

[5] C. G. Kohn, M. J. Alberts, W. F. Peacock, T. J. Bunz, and C. I. Coleman, "Cost and inpatient burden of peripheral artery disease: findings from the national inpatient sample," *Atherosclerosis*, vol. 286, pp. 142–146, Jul. 2019. [Online]. Available: https://linkinghub.elsevier.com/retrieve/pii/S0021915019304538

[6] M. Cai *et al.*, "Temporal trends in incidence rates of lower extremity amputation and associated risk factors among patients using veterans health administration services from 2008 to 2018," *JAMA Network Open*, vol. 4, no. 1, p. e2033953, Jan. 2021. [Online]. Available: https://jamanetwork.com/journals/jamanetworkopen/fullarticle/2775407

[7] J. Allen, "Photoplethysmography and its application in clinical physiological measurement," *Physiological Measurement*, vol. 28, no. 3, pp. R1–R39, Mar. 2007. [Online]. Available: https://iopscience.iop.org/article/10.1088/0967-3334/28/3/R01

[8] R. Avram *et al.*, "A digital biomarker of diabetes from smartphone-based vascular signals," *Nature Medicine*, vol. 26, no. 10, pp. 1576–1582, Oct. 2020. [Online]. Available: https://www.nature.com/articles/s41591-020-1010-5

[9] M. Elgendi *et al.*, "The use of photoplethysmography for assessing hypertension," *npj Digital Medicine*, vol. 2, no. 1, p. 60, Jun. 2019. [Online]. Available: https://www.nature.com/articles/s41746-019-0136-7

[10] R. Avram *et al.*, "Validation of an algorithm for continuous monitoring of atrial fibrillation using a consumer smartwatch," *Heart Rhythm*, vol. 18, no. 9, pp. 1482–1490, Sep. 2021. [Online]. Available: https://linkinghub.elsevier.com/retrieve/pii/S1547527121003180

[11] B. De Ridder, B. Van Rompaey, J. K. Kampen, S. Haine, and T. Dilles, "Smartphone apps using photoplethysmography for heart rate monitoring: meta-analysis," *JMIR Cardio*, vol. 2, no. 1, p. e4, Feb. 2018. [Online]. Available: http://cardio.jmir.org/2018/1/e4/

[12] J. Allen, H. Liu, S. Iqbal, D. Zheng, and G. Stansby, "Deep learning-based photoplethysmography classification for peripheral arterial disease detection: a proof-of-concept study," *Physiological Measurement*, vol. 42, no. 5, p. 054002, May 2021. [Online]. Available: https://iopscience.iop.org/article/10.1088/1361-6579/abf9f3